

# Laser Treated Lines Overlapping on Surface Modification of 304 Stainless Steel

Sahar Sohrabi<sup>a</sup>, Hedieh Pazokian<sup>b,\*</sup> and Mohsen Montazerolghaem<sup>b</sup>

<sup>a</sup>Department of Physics, Iran University of Science and Technology, Tehran, Iran

<sup>b</sup>Photonics and Quantum Technologies Research School, Nuclear Science and Technology Research Institute, Tehran, Iran

Corresponding author email: hpazokian@aeoi.org.ir

Regular Paper-Received: June 15, 2024, Revised: Aug. 16, 2024, Accepted: Aug. 22, 2024, Available Online: Aug. 24, 2024, DOI: 10.61186/ijop.17.2.205

**ABSTRACT**— laser pulse overlapping (LPO) is an important factor affect the behavior of the laser treated surfaces. For laser surface treatment especially at high fluences, the laser beam must be focused to reach the desired fluence. Then laser beam or sample scanning in 2 directions is done to treat a surface area. In this paper, effect of the distance between laser treated lines (scanned in x direction) on the surface properties including morphological changes and wettability modifications of 304 stainless steel is investigated. The results show that the morphology and chemistry of the surface are influenced effectively by changing the overlap between laser treated line on the surface. Then, it should be considered as an important parameter in laser modification of a large surface with focused laser beam.

**KEYWORDS:** Laser-metal interaction, Nanostructures, Pulse overlapping, Stainless steel.

## I. INTRODUCTION

With surface modification, a wide range of chemical, physical and electrical properties of the surface can be developed [1]. On the other hand, nowadays, surface modification is widely used for nanostructured surfaces fabrication [2]. Nanostructured surfaces have various appropriate properties such as antibacterial behavior [3], [4]. There are different methods for nanomodification of a surface, however, laser treatment is considered as a high-efficient method for nanostructured surface fabrication [4], [5].

In laser-material interaction in an air ambient, surface properties (especially absorption coefficient at the laser wavelength) and laser parameters such as laser fluence, repetition rate, number of pulses and the laser pulses overlapping affect the irradiated surface physical and chemical properties [6], [7].

Laser pulse overlapping is an important factor for laser treatment with a scanning beam [7]. The laser beam may overlap in two directions (X, Y) when a large area is process with a focused laser beam or a small beam spot size. Then, the laser beam overlapping in 2 directions affect the laser mater interaction results.

It has shown that laser irradiation overlapping, affects the corrosion resistance of 304 stainless steel [8], [9]. The effect of laser pulse overlapping on the heat affected zone (HAZ) and crystalline properties of stainless steel has been investigated by [10]. Chen *et al.* [11] revealed the effect of scanning speed on the remelted stainless steel sample following laser irradiation. However, none of these papers have investigated the nanostructures formation on surface of the samples and its effect on its wetting properties following laser irradiation with changing the treated lines overlapping. In this paper, effect of the changes between the overlap of the laser treated lines on the morphology and wettability of the surface is investigated.

As it is shown in Fig. 1, the LPO can be described by different parameters such as the distance travelled by two consequent laser pulses ( $b$ ) and the percentage of laser pulse overlapping ( $S\%$ ). It is worth noting that laser beam spot diameter is an important parameter in laser pulses overlapping amount calculation. Parameter  $b$  can be calculated using Eq. (1) [12], [13]:

$$b = \frac{v}{f} \quad (1)$$

where  $v$  is scanning velocity and  $f$  is the laser pulses repetition rate.

On the other hand,  $N$  pulses is required for the laser beam to travel the distance equal to the laser beam diameter ( $2r$ ).  $N$  is dependent on  $b$  and ( $2r$ ) [12]:

$$N = \frac{2r}{b} \quad (2)$$

Finally, the corresponding overlap of each pulse over the spot area can be calculated using Eq. (3) [12], [13]:

$$S_{pulse} = \frac{2r - (n-1)b}{2r} \quad (3)$$

where  $n$  is the number of the pulse. It can be from 1 to  $N$ . Figure 1 shows  $2r$ ,  $b$  and  $S_{pulse}$  for  $n=2$  (blue lines) and  $n=3$  (red lines).

On the other hand, when a material surface is scanned with a laser, several laser pulses interact within a spot area.  $E$ , The total effective energy influences on this area can be calculated by Eq. (4) [12].

$$E = \sum_{n=1}^N S_{pulse} \times e \quad (4)$$

where  $e$  is the energy of the individual laser pulse.

As it is seen, the LPO has significant effect on laser mater interaction with a scanning beam or sample regarding to the total energy deposited on a spot area and the interaction time. On the

other hand, as it was mentioned earlier, the LPO may happen in 2 directions, depends on the laser irradiation parameters.

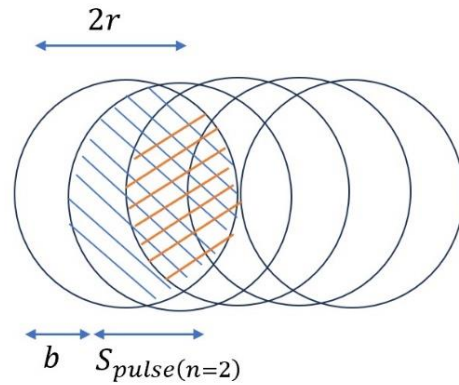


Fig. 1. Laser pulses overlapping parameters. Blue lines show the pulse overlap ( $S_{pulse}$ ) for  $n=2$  and red lines show the pulse overlap for  $n=3$ .

304 stainless steel is a material with several appropriate properties such as good resistance to oxidation, excellent corrosion resistance and good machinability [14], [15] which make it suitable for various industrial applications such as medicine [16]. In our last paper (submitted), we investigated the effect of the LPO on the morphological and antibacterial changes on a 304 stainless steel sample in laser beam scanning direction, called it X. For this purpose, the sample displacement in Y direction (perpendicular to the scanning velocity and in the plane of the sample surface) was chose to be bigger than the laser beam spot size to avoid pulse overlapping in this direction. In this paper, the effect of the pulse overlapping in Y direction is investigated, while, the LPO in X direction remain constant.

## II. MATERIALS AND METHODS

304 stainless steel samples are irradiated by a pulsed Nd-YAG laser with the wavelength of 1064  $\mu\text{m}$ , pulse duration of 16 nanoseconds and at a repetition rate of 10 Hz. Samples were cut in the dimension of 1cm  $\times$  1cm in length and width. Before laser treatment, samples were washed with water and ethanol (98%). The sample was mounted on a X-Y moving stage. All the samples were scanned in X-direction with the velocity of 64 micrometers/second, while the displacement in Y-direction was adjusted to be 100, 150 and 200 micrometers

for different samples. using the translated stage (the laser beam diameter was 250 micrometers). Figure 2 presents the schematic diagram of experimental setup as it was mentioned in our previous paper [17].

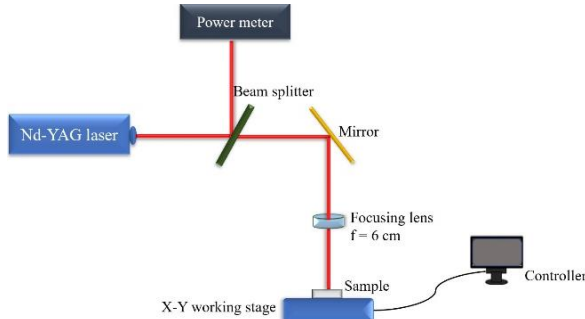


Fig. 2. Schematic diagram of experimental setup. Scanning velocity in X-direction is  $64 \mu\text{m/s}$ , while the displacement of two x-lines is adjusted by the working stage.

For all the samples, the laser fluence was chosen to be  $5 \text{ J/cm}^2$  which is above the ablation threshold fluence ( $3 \text{ J/cm}^2$ ).

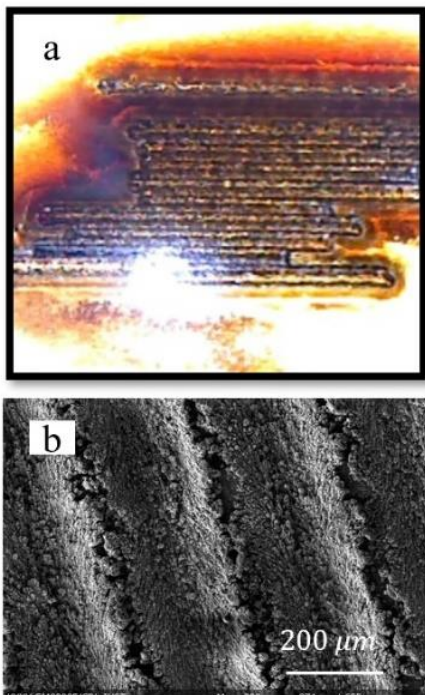


Fig. 3. (a) microscopic and (b) FESEM image of the sample irradiated at the fluence of  $5 \text{ J/cm}^2$ , with scanning velocity of  $64 \mu\text{m/s}$  in X-direction and Y-displacement of  $250 \mu\text{m}$ .

After the irradiation, field emission scanning electron microscopy (FESEM) was used for investigating the shape, size and distribution of the formed micro/nano structures following

laser irradiation. Atomic force microscopy (AFM) was used for surface topography examination. Figure 3 shows typical optical and Scanning electron microscope images of the irradiated sample at the fluence of  $5 \text{ J/cm}^2$  and with Y-displacement of 250 micrometers (equal to the laser beam diameter).

Sessile drop method was used for water contact angle measurement on the non-irradiated and irradiated samples. Sessile drop method for water contact angle entails using a liquid sampler to place a water droplet on the sample and capture its shape with optical microscope. Then, with computer software (ImageJ) the angle between the droplet and the surface can be estimated.

### III. RESULTS AND DISCUSSION

#### A. Laser pulses overlapping value

According to eq (1), (2) and (3),  $b$ ,  $N$  and  $S_{pulse}$  can be calculated in X-direction.  $S_{pulse}$  (for  $n=2$ ) was calculated to be 0.98,  $N$  was 54.68 and  $b$  was 6.4.

Since the scanning velocity is only in X-direction, the laser pulses overlapping amount in Y-direction cannot be calculated using mentioned equations. Therefore,  $b$  in Y-direction was calculated geometrically and according to the amount of beam movement in the Y-direction and the diameter of the laser beam. Then,  $N$  and  $S_{pulse}$  were calculated by Eqs. (2) and (3), respectively. Table. 1 shows the overlapping amount parameters in Y-direction. The sample displacement in Y-direction were 100, 150 and  $250 \mu\text{m}$ . Then, according to the laser beam diameter, in 250 micrometers movement in Y-direction, there is no laser overlapping in Y-direction.

Table 1. Laser pulses overlapping parameters in different displacement in Y-direction.

| Displacement in Y-direction ( $\mu\text{m}$ ) | Spulse (%) | N   |
|---|------------|-----|
| 100   | 71         | 3.5 |
| 150   | 57         | 2.3 |
| 250   | 0          | -   |

As it is obvious, with increasing the displacement in Y-direction, the percentage of laser pulses overlapping decreases. Then, the

number of pulses interact to a constant area between 2 scanned lines in X direction decreases.

### B. Morphology and topography

Figure 4 shows the FESEM images of the non-irradiated and irradiated samples at the mentioned experimental conditions with the displacement of 100, 150 and 250  $\mu\text{m}$  in Y-direction.

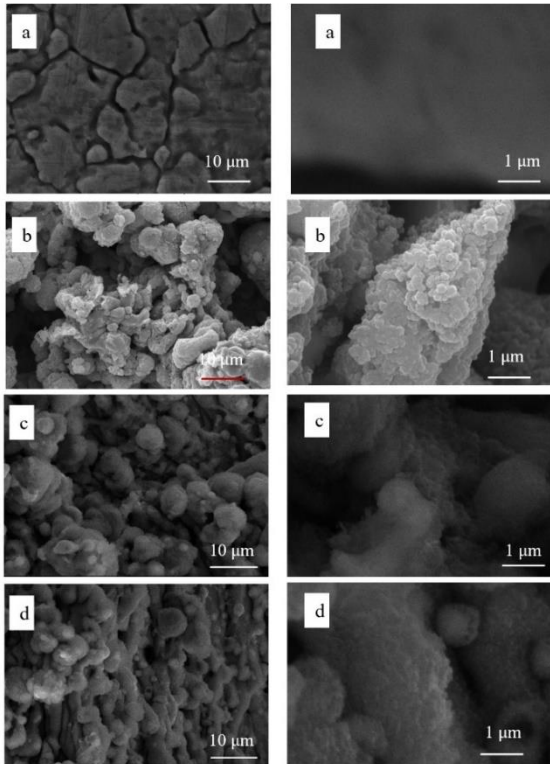


Fig. 4. FESEM images of (a) non-irradiated and irradiated samples at fluence of 5  $\text{J}/\text{cm}^2$  and at a repetition rate of 10 Hz with scanning velocity of 64  $\mu\text{m}/\text{s}$  in X-direction and Y-displacement of (b) 250 (no overlapping in Y-direction), (c) 150 and (d) 100  $\mu\text{m}$  with two different magnifications.

As it is clear from Fig. 4, there are some micro cracks on the non-irradiated stainless steel. Laser treatment of the sample with scanning laser beam in X direction leads to micro structuring of the surface as it can be seen in Fig. 4(a) for the FESEM images of the sample moved 250  $\mu\text{m}$  in Y direction. However, a closer look at the irradiated area shows the nanostructures on the formed microstructures. When the sample moves about 100 and 150  $\mu\text{m}$  in Y direction, the pulse overlapping happen. The value for the LPO is about 57% and 71%, respectively according to the Table. 2.

Although, this overlapping perpendicular to the laser irradiated line in X direction it seems to has not significant effect on microstructure formation, but it is very important in nanoscale.

Figure 5 presents the AFM images of the non-irradiated and irradiated samples at fluence of 5  $\text{J}/\text{cm}^2$  with the pulse repetition rate of 10 Hz with scanning velocity of 64  $\mu\text{m}/\text{s}$  in X-direction and Y-displacement of 100 and 250  $\mu\text{m}$ . As is clear from figure the surface topography of the samples irradiated at the mentioned conditions with displacement in Y-direction of 100 and 250  $\mu\text{m}$  is completely different. The surface irradiated with Y-direction displacement of 100  $\mu\text{m}$  and 150  $\mu\text{m}$  (is not shown) is nano-roughened (Fig. 5(b)) shows a dense nanostructure with the height of about 100 nm, while the height in the sample with no overlapping in Y direction is in the order of 1  $\mu\text{m}$ . On the other hand, in spite of the existence of the nanostructures on the surface, the interaction may occur dominantly between in surface microstructures and the mater. While, nanostructures have significant effect on the mater interaction with surface covered by microstructures with lower height covered by nanostructures.

### C. Wettability

Surface wettability which affected by the surface morphology and chemistry [18], [19], is an important feature of the sample in various applications such as medicine. Superhydrophilic surfaces have wide practical applications in biomedical [20], oil-water separation [21] and so on. As it was shown in the last section, LPO has significant effect on surface nanostructures. Here, the water droplet contact angle on the surface was investigated to study the effect of the formed structures on the surface. Table 2, shows the wettability of the non-irradiated and irradiated samples at the mentioned conditions.

It is obvious from the table that the samples irradiated at the fluence of 5 with 100 and 150  $\mu\text{m}$  displacement in Y-direction, show superhydrophilic behavior. While, the sample with no LPO in Y direction is hydrophobic. According to the Wenzel theory, nanostructures



formation on the hydrophilic sample causes the surface to turn into the more hydrophilic one [22]. On the other hand, the water droplet interacts with higher hierarchical structures formed on the sample with Y-displacement of 250 micrometers, which cause air-trapping [23] in the formed structures followed by increasing the water contact angle of the sample.

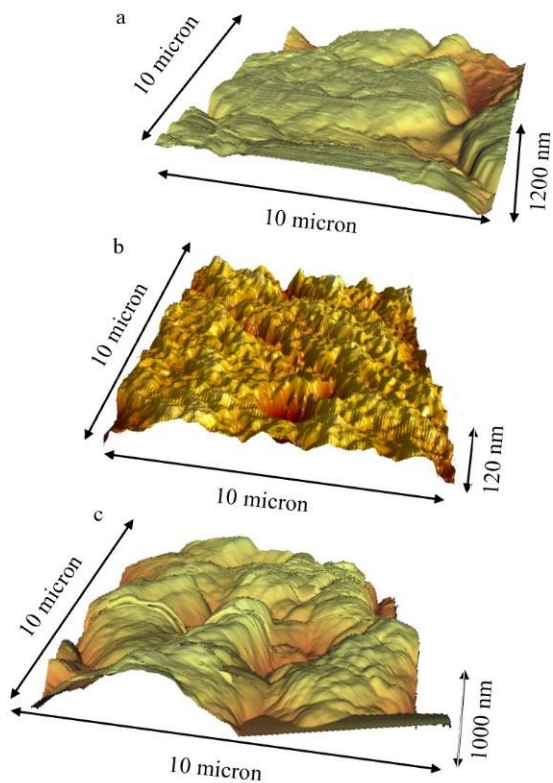


Fig. 5. AFM images of (a) non-irradiated and irradiated samples at fluence of 5 J/cm<sup>2</sup> and at a repetition rate of 10 Hz with scanning velocity of 64 μm/s in X-direction and Y-displacement of (b) 100, and (c) 250 μm.

Table 2. Wettability of non-irradiated and irradiated samples in different conditions

| Y displacement (μm) | Microscopic image of water droplet on the surface | Water contact angle (degree) |
|---------------------|---|------------------------------|
| Pristine            |   | 50                           |
| 100                 |   | 0                            |
| 150                 |   | 0                            |
| 250                 |   | 120                          |

IV.CONCLUSION

In this paper, stainless steel samples were irradiated by a pulsed Nd-YAG laser (1064 nm and 16 ns) at the fluence of 5 J/cm<sup>2</sup> with scanning velocity of 64 μm/s in X-direction and Y-displacement of 100, 150 and 250 μm between two consequent X-scanning lines. The results show that LOP in the Y-direction has significant effect on the morphological changes on the surface at nanoscale in the mentioned irradiation parameters. This result is very important in surface interactions for different application. Therefore, LPO is a very principal factor for the laser mater processing and must be optimized for desirable application.

REFERENCES

[1] M. Castillejo, M. Martín, M. Oujja, J. Santamaría, S. Diego, R. Torres, A. Manousaki, V. Zafiropulos, O.F. Van den Brink, R.M. Heeren, and R. Teule, “Evaluation of the chemical and physical changes induced by KrF laser irradiation of tempera paints,” J. Cult. Herit., Vol. 4, pp. 257-263, 2003.

[2] C. Bae, H. Shin, and K. Nielsch, “Surface modification and fabrication of 3D nanostructures by atomic layer deposition,” Mater. Res. Soc. (MRS) Bulletin, Vol. 36, pp. 887-897, 2011.

[3] L. Xia. “Importance of nanostructured surfaces,” Bioceramics. Elsevier, pp. 5-24, 2021.

[4] S. Sohrabi, H. Pazokian, B. Ghafary, and M. Mollabashi, “Super-hydrophilic nano-structured surface with antibacterial properties,” Opt. Mater. Express, Vol 14, pp. 116-124, 2023.

[5] G. Ou, P. Fan, H. Zhang, K. Huang, C. Yang, W. Yu, H. Wei, M. Zhong, H. Wu, and Y. Li, “Large-scale hierarchical oxide nanostructures for high-performance electrocatalytic water splitting,” Nano Energy, Vol. 35, pp. 207-214, 2017.

[6] M. Stafe, A. Marcu, and N. Puscas. *Pulsed laser ablation of solids*, Springer, Vol. 10, PP. 978-983, 2014.

[7] S. Ravi-Kumar, B. Lies, X. Zhang, H. Lyu, and H. Qin, “Laser ablation of polymers: a review,” Polymer Int., Vol. 68, pp. 1391-1401, 2019.

- [8] W. Pacquentin, N. Caron, and R. Oltra, "Nanosecond laser surface modification of AISI 304L stainless steel: Influence the beam overlap on pitting corrosion resistance," *Appl. Surf. Sci.*, Vol. 288, pp. 34-39, 2014.
- [9] C.Y. Cui, X.G. Cui, Y.K. Zhang, Q. Zhao, J.Z. Lu, J.D. Hu, Y.M. Wang. "Microstructure and corrosion behavior of the AISI 304 stainless steel after Nd: YAG pulsed laser surface melting," *Surf. Coat. Technology*, Vol. 206, pp. 1146-1154, 2011.
- [10] L.J Yang, J. Tang, M.L. Wang, Y. Wang, and Y.B. Chen, "Surface characteristic of stainless-steel sheet after pulsed laser forming," *Appl. Surf. Sci.*, Vol. 256, pp. 7018-7026, 2010.
- [11] J. Ghorbani, J. Li, A.K. Srivastava, "Application of optimized laser surface remelting process on selective laser melted 316L stainless steel inclined parts," *J. Manuf. Process.*, Vol. 56, pp. 726-734, 2020.
- [12] H. Pazokian, "Theoretical and experimental investigations of the influence of overlap between the laser beam tracks on channel profile and morphology in pulsed laser machining of polymers," *Optik*, Vol. 171, pp. 431-436, 2018.
- [13] N.B. Dahotre, S.R. Paital, A.N Samant, and C. Daniel, "Wetting behaviour of laser synthetic surface microtextures on Ti-6Al-4V for bioapplication," *Philos. Transact. A Math. Phys. Eng. Sci.*, Vol. 368, pp. 1863-1889, 2010.
- [14] A. Kumar, R. Sharma, S. Kumar, and P. Verma, "A review on machining performance of AISI 304 steel," *Mater. Today*, Vol. 56, pp. 2945-2951, 2022.
- [15] M. Kaladhar, K.V. Subbaiah, and CH.S. Rao, "Machining of austenitic stainless steels—a review," *Int. J. Mach. Mach. Mater.*, Vol. 12, pp. 178-192, 2012.
- [16] R.J. Narayan, *Medical Application of Stainless steels*, ASM Handbook, Vol. 23, pp.199-210, 2012.
- [17] V. Khranovskyy, T. Ekblad, R. Yakimova, and L. Hultman, "Surface morphology effects on the light-controlled wettability of ZnO nanostructures," *Appl. Surf. Sci.*, Vol. 258, pp. 8146-8152, 2012.
- [18] V. Khranovskyy, T. Ekblad, R. Yakimova, and L. Hultman, "Surface morphology effects on the light-controlled wettability of ZnO nanostructures," *Appl. Surf. Sci.*, Vol. 258, pp. 8146-8152, 2012.
- [19] C.G. Jothi Prakash, and R. Prasanth, "Approaches to design a surface with tunable wettability: a review on surface properties," *J. Mater. Sci.*, Vol. 56, pp.108-135, 2021.
- [20] E.J. Falde, S.T. Yohe, Y.L. Colson, and M.W. Grinstaff, "Superhydrophobic materials for biomedical applications," *Biomater.*, Vol. 104, pp. 87-103, 2016.
- [21] Z. Xiong, H. Lin, Y. Zhong, Y. Qin, T. Li, and F. Liu, "Robust superhydrophilic polylactide (PLA) membranes with a TiO<sub>2</sub> nano-particle inlaid surface for oil/water separation." *J. Mater. Chem. A*, Vol. 5, pp. 6538-6545, 2017.
- [22] H. Li, X. Feng, and K. Zhang, "Study of the classical cassie theory and Wenzel theory used in nanoscale," *J. Bionic Eng.*, Vol. 18, pp. 398-408, 2021.
- [23] H.Y. Erbil and C. Elif Cansoy, "Range of applicability of the Wenzel and Cassie–Baxter equations for superhydrophobic surfaces," *Langmuir*, Vol. 25, pp. 14135-14145, 2009.



**Sahar Sohrabi** was born in Semnan, Iran. She received her B.Sc., M.Sc., and PhD (2024) degrees in atomic and molecular physics from Iran University of Science and Technology, Tehran, Iran, in 2015, 2017, 2024, respectively.

Her current research interests include laser-material interaction, laser induced surface phenomena and lasers in medicine and biology.



**Hedieh Pazokian** was born in Tehran, Iran. She received her B.Sc. degree in physics from

Semnan University in 2004. She obtained M.Sc. and PhD degrees in physics from Iran University of Science and Technology, Tehran, Iran, in 2006 and 2011, respectively.

Her current research interest includes laser-material interaction, laser induced graphene, optical materials fabrication, optofluidic, laser nanotechnology and nano photonics.



**Mohsen Montazerolghaem** was born in Esfahan, Iran.

His current research interest include laser-material interaction, optoelectronic devices, optical communication and network and laser science.

**THIS PAGE IS INTENTIONALLY LEFT BLANK.**